Biol Invasions (2023) 25:61–78
https://doi.org/10.1007/s10530-022-02891-7

ORIGINAL PAPER

Physiochemical responses of *Ailanthus altissima* under the challenge of *Verticillium dahliae*: elucidating the decline of one of the world's worst invasive alien plant species

Claudia Pisuttu · Ermes Lo Piccolo · Luca Paoli · Lorenzo Cotrozzi · Cristina Nali · Elisa Pellegrini · Giacomo Lorenzini

Received: 1 January 2022 / Accepted: 27 July 2022 / Published online: 16 August 2022

Abstract Natural infections of *Verticillium* spp. (Fungi, Ascomycota) on *Ailanthus altissima* have suggested to consider the biological control as a promising strategy to counteract this invasive plant, which is otherwise difficult to control by traditional mechanical and chemical treatments. Verticillium wilt is able to lead plants to death, throughout a pathogenic mechanism including vessel occlusions and production of degrading enzymes and phytotoxins. In this study, a 10 weeks open air pot experiment was set to investigate the ecophysiological and biochemical responses of *Ailanthus* trees artificially inoculated in the trunk with the *V. dahliae* strain VdGL16, previously isolated in Central Italy from the same host. Inoculated plants showed visible injuries starting from 2 weeks post inoculation (wpi), that progressively developed until a final severe defoliation. The fungal infection rapidly compromised the plant water status, and photosynthesis was impaired due to both stomatal and mesophyll limitations from 4 wpi, with subsequent detrimental effects also on PSII activity. Moreover, the disease altered the translocations of nutrients, as confirmed by cation and carbohydrate contents, probably due to a consumption of simple sugars and starch reserves without replacement of new photosynthesized. An accumulation of osmolytes (abscisic acid and proline) and phenylalanine (a precursor of phenylpropanoids) was also reported at 8 wpi, this being a response mechanism that needs to be further elucidated. However, the activation delay of such defence strategy inevitably did not avoid the premature defoliation of plants and the decline of physiochemical parameters, confirming the key role of *Verticillium* in *Ailanthus* decay.

Keywords Mycoherbicide · Osmolytes · Photosynthesis · Primary metabolites · Tree of heaven · Wilt disease

C. Pisuttu · E. Lo Piccolo · L. Cotrozzi · C. Nali · E. Pellegrini (✉) · G. Lorenzini
Department of Agriculture, Food and Environment, University of Pisa, Via del Borghetto 80, 56124 Pisa, Italy
e-mail: elisa.pellegrini@unipi.it

C. Pisuttu
e-mail: claudia.pisuttu@phd.unipi.it

E. Lo Piccolo
e-mail: ermes.lopiccolo@agr.unipi.it

L. Cotrozzi
e-mail: lorenzo.cotrozzi@unipi.it

C. Nali
e-mail: cristina.nali@unipi.it

G. Lorenzini
e-mail: giacomo.lorenzini@unipi.it

L. Paoli
Department of Biology, University of Pisa, Via Ghini 13, 56126 Pisa, Italy
e-mail: luca.paoli@unipi.it

Introduction

Ailanthus altissima (Mill.) Swingle (Simaroubaceae; hereafter *Ailanthus*), also known as 'tree of heaven', is a tree species native to East Asia that has been designated as one of the "100 of the World's Worst Invasive Alien Species" by the IUCN Invasive Species Specialist Group (Kowarik et al. 2021), after becoming an undesired plant in many world regions such as North America (Schall and Davis 2009a), South Africa (Walker et al. 2017) and Europe (Kowarik and Säumel 2007; Nentwig et al. 2018). Firstly, introduced to Europe in the 1740s (Hu 1979), mainly as ornamental species in several cities because of its tolerance to urban stressful conditions and its resistance to herbivory (Kowarik and Säumel 2007), *Ailanthus* has since spread so widely and uncontrollably that from August 2019 it has also been included among the Invasive Alien Species (IAS) of Union Concern (Kowarik et al. 2021).

The high invasiveness of *Ailanthus* is not only due to its resistance/tolerance to most abiotic and biotic stresses, but also to its strong efficacy in both gamic reproduction (e.g., it can produce much more than 300,000 samaras per tree in a single growing season, and samaras, being flat twisted and very light, are well suited for long-range wind dispersal; Kowarik and Säumel 2007) and agamic propagation through aggressive sprouting of roots and stems (Schall and Davis 2009a), as well as to an extremely rapid growth, especially during the youth stages. In addition, it is a strong producer of quassinoid compounds that possess phytotoxic allelopathic properties and are able to inhibit germination and growth of several plant species (De Feo et al. 2003; Webster et al. 2006). Therefore, although it is shade-intolerant, *Ailanthus* severely outcompetes forest native species and challenges biodiversity in areas where it occurs, especially in those climates subjected to increasing drought frequency and severity (Knüsel et al. 2015; Montecchiari et al. 2020). However, the areas mostly challenged worldwide by *Ailanthus* pressure are likely represented by the urban and peri-urban sites where this invasive species largely spreads, given its ability to colonize these environments with a particular aptitude for occupying transportation corridors, and its frequent and substantial damages to urban infrastructures and archaeological sites (Trotta et al. 2020; Fogliatto et al. 2020).

The growth characteristics of *Ailanthus* make it particularly difficult to control. Preventive methods should be adopted to avoid/reduce the spread of the species through seed dispersal by limiting, for example, the movement of soil from infested areas and especially by prioritising the control of large female trees to reduce seed rain (EPPO 2020). Although several mechanical (e.g., pulling and digging, tree felling, girdling, mowing and chipping aboveground plant parts and burning; Schall and Davis 2009a) and chemical methods have been attempted to control *Ailanthus* invasions, these strategies are usually ineffective, even stimulating stump and root re-sprouting, especially if applied singularly (DiTomaso and Kyser 2007; Badalamenti et al. 2015). Differently, the simultaneous or consecutive applications of systemic chemical herbicides, with mechanical practices, are commonly more effective, mainly because chemicals translocated to the roots tackle vegetative renewal (DiTomaso and Kyser 2007; EPPO 2020; Fogliatto et al. 2020). However, also chemical herbicides have been shown to be generally ineffective against the re-sprouting ability of *Ailanthus*. Moreover, their use is expensive and laborious, not to mention their negative impacts on non-target vegetation (being them non-selective) and ecosystems, which is the main reason of the increasing restrictions in the use of such chemical products (Pisuttu et al. 2020a). So, for instance, glyphosate, the most frequently used herbicide both worldwide and in the EU which has been used for several decades is currently approved in the EU until 15 December 2022 (https://ec.europa.eu/food/plants/pesticides/approval-active-substances/renewal-approval/glyphosate_en), but many countries have placed important restrictions on its use. Consequently, the control of *Ailanthus* is a major concern because long-term methods able to adequately limit its invasion are lacking so far.

Interestingly, some *Ailanthus* decay due to soil-borne fungal pathogens of the genus *Verticillium* (Ascomycota, Plectosphaerellaceae) have been reported in the last years in several areas in the USA and Europe, so proposing the biological control as a possible strategy to successfully counteract the apparently irrepressible spread of this invasive species (Sheppard et al. 2006). Specifically, two main endemic *Verticillium* species, i.e., *V. nonalfalfae* Inder. and *V. dahliae* Kleb., have been reported to be able to infect *Ailanthus* and lead it to death in a

few years, and further infect neighbouring healthy trees by intraspecific root grafting (O'Neal and Davis 2015). The virulence and the spread of these fungal species seem strictly related to the climatic conditions: infections due to both *Verticillium* species have been found in countries characterized by temperate climate such as Pennsylvania, Virginia, and Ohio in the USA (Schall and Davis 2009a; Snyder et al. 2013; Rebbeck et al. 2013), as well as in Austria in Europe (Maschek and Halmschlager 2017), where *V. nonalfalfae* is more aggressive (Brooks et al. 2020) and best adapted than *V. dahliae*. Conversely, infections caused only by *V. dahliae* have been reported in Hungary (Izsépi et al. 2018) and in different Mediterranean regions (i.e., Greece, Italy, and Spain; Skarmoutsos and Skarmoutsou 1998, Longa et al. 2019, Pisuttu et al. 2020a, Moragrega et al. 2021) where *V. nonalfalfae* has been rarely reported also on other hosts, because its optimum growth temperature is around 22 °C and is infrequently present outside the 10–27 °C range (Maschek and Halmschlager 2017). These reports thus suggest to focus on the role of *V. dahliae* (able to survive up to 30 °C; Pegg and Brady 2002), currently the only natural endemic enemy reported as able to limit *Ailanthus* invasion in the warmer environments.

In accordance with the above outcomes, our research group recently provided evidence of the presence of a previously unreported wilt disease of *Ailanthus* in Tuscany (Central Italy), then attributed to *V. dahliae*. The isolated strain (i.e., VdGL16) was proven to be virulent towards both *Ailanthus* seedlings from several Italian provenances and adult trees, not infectious in trees or shrubs of economic or landscape interest, whereas only a few herbaceous species of horticultural and forage concern resulted susceptible among the 40 non-target species/varieties/cultivars tested (Pisuttu et al. 2020a). This study also allowed to develop on optimal inoculation method for adult trees, both in terms of infection efficacy and environmental safety (i.e., to avoid accidental spread of conidial suspension). *Verticillum dahliae* was thus proposed as the so far best candidate for an efficient, low cost and sustainable control of the invasive *Ailanthus*, especially in urban and peri-urban Mediterranean areas. However, it was also highlighted the need not only to further test the susceptibility of other non-target species (to be clear, *V. dahliae* can infect more than 200 different hosts including crops of economic and landscape importance in Italy and in the Mediterranean basin such as *Olea europaea*; Fradin and Thomma 2006, Mulero-Aparicio et al. 2020), but also to better understand the responses of *Ailanthus* under the challenge of *V. dahliae*, in order to elucidate the pathogenic mechanisms behind the effectiveness of this biocontrol agent.

Thus, the present study aimed to broadly investigate at macroscopic, ecophysiological and biochemical levels the responses of *Ailanthus* inoculated with *V. dahliae* strain VdGL16. Specifically, we postulated that (i) *V. dahliae* infection simulates drought stress, but following a more complex and rapid pathogenic mechanism due to the inclusion of cell-wall-degrading enzymes, toxic compounds and elicitors produced by the fungus (Fradin and Thomma, 2006), and (ii) even if *Ailanthus* is able to activate defence responses against *V. dahliae*, its strong invasiveness is progressively reduced by the fungal disease, and its death is essentially unavoidable in the presence of the proposed biocontrol agent.

Materials and methods

Biological material and experimental design

In June 2019, 4-years-old saplings of *A. altissima* were purchased from a commercial nursery (Milan, Italy, 45°27′68″ N, 9°09′34″ E, 120 m a.s.l.) and transferred to the field-station of San Piero a Grado (Pisa, Italy, 43°40′48″ N, 10°20′46″ E, 2 m a.s.l.) owned by the Department of Agriculture, Food and Environment (DAFE) of the University of Pisa. Here, plants were directly transplanted into 10-L plastic pots filled with a mixture of a peat and clay standard soil (Topfsubstrat ED 63 T grob, Einheitserde, Sinntal-Altengronau, Sinntal, Germany; 34% organic C, 0.2% organic N and pH of 5.8–6.8) and coconut fibres (3:1), and maintained well-watered (i.e., at field capacity) and under field conditions until the end of the experiment.

Verticillium dahliae strain VdGL16 (deposited in GenBank with the accession number MK474459), initially isolated from a naturally infected *Ailanthus* scion and preserved in the DAFE-culture collection (Pisuttu et al. 2020a), was grown on potato dextrose agar (PDA, 39 g L^{-1}; Sigma-Aldrich, Milan, Italy) amended with streptomycin sulphate (0.1 g L^{-1},

Gold Biotechnology, Saint Louis, MO, USA) in Petri dishes (∅ 9 cm) incubated for two consecutive weeks at 23 °C and a 12 h photoperiod. Liquid cultures of *V. dahliae* were prepared in Erlenmeyer flasks (0.5 L) containing Czapek Dox Broth (35 g L^{-1}; Sigma-Aldrich, Milan, Italy) and incubated for 3 days in an orbital shaker (711 CT, Asal, Milan, Italy) set at 150 rpm and kept under room conditions. Conidial suspensions were obtained by filtering liquid cultures through three layers of sterile cheesecloths. According to previous works (Schall and Davis, 2009a, b; Kasson et al. 2015; Maschek and Halmschlager, 2018, Pisuttu et al., 2020a) inoculum concentration was adjusted to approximately $0.8–1 \times 10^7$ conidia mL^{-1} by a Bürker hemocytometer chamber (Henneberg-Sander, Giessen Lützellinden, Germany). The conidial suspension was used for stem inoculations reported below.

On 11th June 2020, 20 plants were randomly selected for uniformity of height (ca. 3 m), habitus and trunk diameter (on average of 12 cm) and stem-inoculated at breast height, according to Pisuttu et al. (2020a). Trunks were punched with an electric drill mounting a sterilized drill bit, so to produce a 6 mm hole (4 cm length) slightly tilted downwards. Afterwards, using micropipettes, 5 mL of the abovementioned conidial suspension were injected inside the holes of 10 randomly selected plants (*V. dahliae*-inoculated), while 5 ml of a sterile Czapek solution were injected inside the holes of the other 10 plants (controls). A rectangular Parafilm M® laboratory film sheet was used for impeding the outflow of the conidial suspension or the Czapek solution. Plants were randomly positioned within the experimental area and repositioned every week to avoid position effects. The daily average, maximum and minimum air temperatures and total precipitation throughout the entire period of the experiment (10 weeks), recorded by an automatic meteorological station located near the experimental site (Coltano, Pisa; 43°37′58″ N, 10°22′55″ E, 2 m a.s.l) were 22.9, 28.5 and 17.2 °C, and 113 mm, respectively. These data were in accordance with those of the 2000–2019 historical series provided by the Hydrological Service of Tuscany Region (Fig. 1).

Verticillium colonization in inoculated *Ailanthus* trees was verified by re-isolating the pathogen from plant tissues. Briefly, petioles of symptomatic leaves were cut in 1-cm pieces, disinfected in sodium

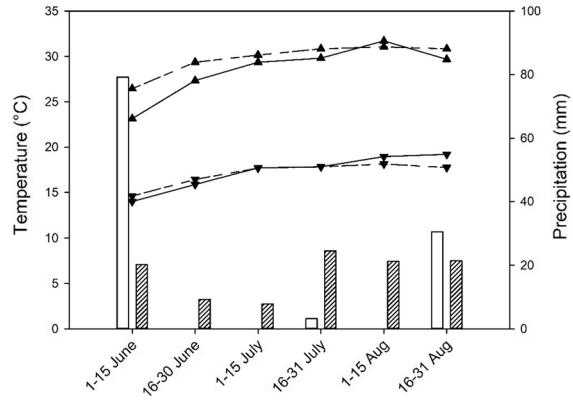

Fig. 1 Climograph of biweekly maximum (Black up-pointing triangle) and minimum (Black down-pointing triangle) air temperatures (°C) and precipitations (mm; bars) referred to the experimental period (solid line; data are from an automatic meteorological station located near the experimental site) or the 2000–2019 historical series (dotted line; data are from the Hydrological Service of Tuscany Region)

hypochlorite (0.5%) for 5 min, rinsed twice with sterile distilled water, gently wizened and finally placed on PDA in Petri dishes (∅ 9 cm), until the development of fungal structures. After 2 weeks, a morphologic identification of *V. dahliae* colonies was carried out using a stereo microscope (Leica S9, Leica Mycrosystems, Milan, Italy; magnification 40×) and an optical microscope (Leica DM 4000B, Leica Mycrosystems; magnification 400×).

Measurements were carried out at 0, 2, 4, 6, 8 and 10 weeks post inoculation (wpi) on all selected plants (i.e., 10 *V. dahliae*-inoculated and 10 controls). The severity of *V. dahliae* infection was assessed on all leaves present at each time of analysis, whereas physiological and biochemical analyses were carried out on at least three mature, totally expanded and asymptomatic leaves per plant, randomly selected in the middle of the foliage. Chlorophyll (Chl) *a* fluorescence measurements were not collected at 2 wpi because no significant *V. dahliae*-induced variations were observed for other investigated physiological parameters at this time of analysis; whereas A/C_i response curves were collected at 6 and 8 wpi, after the occurrence of significant *V. dahliae*-induced variations of gas exchange parameters firstly reported at 4 wpi (see below). At each measurement time, leaf tissues were collected, divided into aliquots, immediately frozen in liquid nitrogen and then stored

at − 80 °C until biochemical analyses. All measurements and leaf collections were performed between 10.00 a.m. and 3.00 p.m.

Assessment of disease severity progress

Disease severity was calculated using an ordinal 0–4 rating system according to the percentage of affected leaves (0 = no symptoms; 1 = 1–33%; 2 = 34–66%; 3 = 67–99%; 4 = dead plant; Prieto et al. 2009). The Area Under the Disease Progress Curve (AUDPC) was determined using the formula reported in Simko and Piepho (2012):

$$AUDPC = \sum_{i=1}^{n-1} \frac{y_i + y_{i+1}}{2} \times \left(t_{i+1} - t_i\right)$$

where y_i is the rate of disease severity determined as described above at the *ith* observation, t_i is time (in days) at the *i*th observation, and n is the total number of observations.

Ecophysiological and water status analyses

Net CO_2 assimilation rate (A), stomatal conductance (g_s) and intercellular CO_2 concentration (C_i) were determined using a portable infrared gas analyser (Li-Cor Inc., Lincoln, NE, USA) equipped with a 2 × 3 cm leaf cuvette operating at 400 µmol mol^{-1} (ambient) CO_2 concentration and 1500 µmol m^{-2} s^{-1} of saturating light. The temperature and relative humidity inside the leaf cuvette were 30 °C and around 45%, respectively. Using the same instrumentation and settings, A/C_i curves were also constructed by adjusting the CO_2 concentration inside the leaf chamber to 400, 200, 150, 50, 400, 600, 800, 1000, 1200, and 1500 µmol mol^{-1}. The CO_2 compensation point in absence of respiration (Γ*) was assumed to be 44.04 at 30 °C (Bernacchi et al. 2002). Maximum rate of carboxylation (V_{cmax}) and electron transport obtained at saturating light (J_{1500}) were calculated according to Long and Bernacchi (2003), based on the model of Farquhar et al. (1980).

Chlorophyll *a* fluorescence emission was measured by a Plant Efficiency Analyzer—Handy PEA (Hansatech Ltd., Norfolk, UK). Each selected leaf was dark adapted for 10 min with a clip randomly placed over its surface and then illuminated for 1 s with a 3000 µmol m^{-2} s^{-1} saturating excitation pulse of red light (650 nm) provided by a LED light source included into the fluorimeter. Fluorescence induction curves were recorded up to 1 s. Up to 20 fluorescence curves were recorded per each individual and analysed by means of the JIP-test (Strasser et al. 2000; Stirbet and Govindjee 2011), which is used to translate original fluorescence data to biophysical parameters that quantify energy fluxes and their ratios, physiological states, conformation, and the overall photosynthetic performance of the samples. The 'vitality' of the samples was summarized by the maximum quantum yield of primary photochemistry as inferred from fluorescence data: $\varphi_{Po} = (F_M - F_0)/F_M = F_V/F_M$. In addition to this classical indicator, the so called performance index (PI_{ABS}) was calculated from another set of equations: $\gamma_{RC}/(1-\gamma_{RC}) \cdot \varphi_{Po}/(1-\varphi_{Po}) \cdot \psi_{Eo}/(1-\psi_{Eo})$, where, $\gamma_{RC} = Chl_{RC}/Chl_{total}$ is the probability that a PSII Chl molecule functions as reaction centre (RC); $\gamma_{RC}/(1-\gamma_{RC})$ is approximated in the JIP-test by RC/ABS, with ABS/RC the inferred absorbed energy flux (ABS) per active RC of PSII; $\varphi_{Po} = TR_0/ABS$ ($= F_V/F_M$) is the inferred maximum of quantum yield of primary photochemistry; $\psi_{Eo} = ET_0/TR_0$ is the probability that an electron moves further than the electron acceptor QA (Strasser et al. 2000; Stirbet and Govindjee 2011). The effects of *V. dahliae* inoculation were further considered by means of transient curves. Fast fluorescence kinetics typically outline a curve: when the curve is plotted on a log-time axis, a typical sequence of steps called O–J–I–P, each corresponding to its changing inclination, is outlined (Strasser et al. 2000). The minimal fluorescence F_0 is measured at 50 µs and corresponds to O, the J-step is recorded at 2 ms, the I-step at 30 ms and P-step at about 300 ms, generally in correspondence of maximal fluorescence F_M.

Leaf water potential (Ψ_{LW}) was measured using a Scholander-type pressure chamber (model 600, PMS Instrument, Albany, NY, USA), using the precautions of Turner and Long (1980). Leaf osmotic potential ($\Psi_{L\pi}$) was converted from osmolality (using the Van't Hoff equation) determined by a VAPRO® Vapor Pressure Osmometer (model 5600, EliTechGroup, Puteaux, France), according to Cotrozzi et al. (2020). Relative water content (RWC) was calculated as (FW-DW)/(TW-DW) × 100, where FW is the fresh weight, TW is the turgid weight after rehydrating samples for 24 h in distilled water, and DW is the dry weight after oven drying samples at 80 °C for 72 h.

Biochemical analyses

Photosynthetic and accessory pigments were measured according to Cotrozzi et al. (2017). About 0.1 g of leaf tissue were extracted with 1 mL of 100% HPLC-grade methanol and incubated overnight at 4 °C in the dark. Samples were centrifuged for 15 min at 16,000×*g* at 4 °C and the supernatant was filtered through 0.2 µm Minisart® SRT 15 aseptic filters, and immediately analysed. Pigments were determined by Ultra-High Performance Liquid Chromatography (UHPLC) using a Dionex UltiMate 3000 system (Thermo Scientific, Waltham, MA, USA) equipped with a reverse-phase Agilent column (ZORBAX Eclipse plus C18, 5 µm particle size, 4.6 mm internal diameter×150 mm length; Agilent Technologies, Inc., Santa Clara, CA, USA) kept at 25 °C. The pigments were eluted using 100% solvent A (acetonitrile/methanol, 75/25, v/v) for the first 14 min to elute all xanthophylls, followed by a 1.5 min linear gradient to 100% solvent B (methanol/ethylacetate, 68/32, v/v), 15 min with 100% solvent B, which was pumped to elute Chl *b* and *a* and β-carotene, followed by 2 min linear gradient to 100% solvent A. The flow-rate was 1 mL min^{-1}. The column was allowed to re-equilibrate in 100% solvent A for 10 min before next injection. The pigments were detected by their absorbance at 445 nm with a Dionex UVD 170 U UV–Vis detector (Thermo Scientific). To quantify the content of pigments, known amounts of pure authentic standards were injected into the UHPLC system and equations, correlating peak area to the concentration of pigments, were formulated. Chromatographic data were processed and recorded by Chromeleon Chromatography Management System software, version 7.2.10-2019 (Thermo Scientific).

Key mineral elements (i.e., Na^+, K^+, Mg^{2+}, Ca^{2+}) were determined by a Dionex Aquion Ion Chromatography System (Thermo Scientific) equipped with a Dionex Cation Self-Regenerating Suppressor CSRS™ 300 and a 4×250 mm Dionex IonPac™ CS12A column Thermo Fisher Scientific, Waltham, MA, USA), provided with a 4×50 mm Dionex IonPac™ CG12A pre-column (Thermo Scientific), according to Calzone et al. (2020). Around 0.1 g of leaf tissue were suspended in 1 mL of 100% HPLC-demineralized water, shaken for 15 min and centrifuged at 2100×*g* for 10 min. After filtration through 0.2 µm Minisart® SRT 15 aseptic filters, the supernatant was tenfold diluted with 100% HPLC-demineralized water and eluted with 20 mM methansulfonic acid. The flow rate was 1 mL min^{-1}. Data are shown as K^+/Na^+, K^+/Ca^{2+} and K^+/Mg^{2+} ratios.

Abscisic acid (ABA) content was determined after extracting 0.1 g of leaf tissue in 1 mL of distilled water, and the resulting supernatant was furtherly diluted 10 times. The determination of ABA was performed at 415 nm with a fluorescence/absorbance microplate reader (Victor3 1420 Multilabel Counter, Perkin Elmer, Waltham, MA, USA), by using the Phytodetek® Immunoassay Kit for ABA (Agdia Elkhart, IN, USA).

Soluble carbohydrate contents were determined according to Pellegrini et al. (2015), with slight modifications. About 50 mg of leaf tissue were extracted with 1 mL of 100% HPLC-demineralized water in a water bath at 60 °C for 60 min. Samples were centrifuged for 15 min at 16,000×*g* at 4 °C and the supernatant was filtered through 0.2 µm Minisart® SRT 15 aseptic filters. Soluble carbohydrates were determined by the same UHPLC system reported above equipped with a Repromer H column (9 µm particle size, 8 mm internal diameter×300 mm length; Dr Maisch, Ammerbuch, Germany), provided with a pre-column (9 µm particle size, 8 mm internal diameter×20 mm length; Dr Maisch), kept at 30 °C. The isocratic mobile phase was 9 mM sulphuric acid, eluted at a flow rate of 1 mL min^{-1}. Soluble carbohydrates were detected by their absorbance at 210 nm with a differential refractometer (Shodex, West Berlin, NJ, USA). To quantify soluble carbohydrate contents, known amounts of pure standard were injected into the HPLC system. An equation correlating the peak area to each soluble carbohydrate standard concentration was formulated using the software reported above. The sum of sucrose, glucose and fructose, was considered as a measure of total soluble carbohydrate content (Tot car).

Starch content was determined using the commercial kit K-TSTA (Megazyme, Wicklow, Ireland) according to the manufacturer's protocol. Around 0.1 g of pellet were suspended in 80% aqueous ethanol (v/v). The α-amylase hydrolysed the total starch in maltodextrins and, subsequently, two enzymatic procedures were carried out (i) to idrolyse maltodextrins to D-glucose (by using amyloglucosidase) and (ii) to oxidase D-glucose in gluconate (by using glucose oxidase). During this reaction, a production of

a quinoneimine dye occurred with the concomitant release of one mole of hydrogen peroxide, which was quantitatively measured in a colorimetric reaction employing peroxidase. Absorbance at 510 nm was determined using the fluorescence/absorbance microplate reader reported above.

Amino acid (AA) contents were measured according to Fish (2012). Around 0.1 g of leaf tissue were extracted with 1 mL of 100% HPLC-demineralized water and the supernatant filtered through 0.2 µm Minisart® SRT 15 aseptic filters, was analysed by the same UHPLC system reported above equipped with a Zorbax Eclipse AAA column (5 µm particle size, 4.6 mm internal diameter × 150 mm length; Agilent, Milan, Italy) kept at 40 °C. A pre-column derivatization was performed by neutralizing samples in 0.4 M borate buffer (pH 10.2) to ensure that the amino terminus of each AA was neutralized. Primary amines were then reacted with o-phthaldehyde (OPA), and secondary amines (such as proline) were reacted with 9-fluorenylmethylchloroformate (FMOC-Cl). UHPLC analytical conditions were as follows: 100% solvent A [demineralized water 40 mM sodium phosphate dibasic buffer (pH 7.8)] for the first 18 min followed by a 1 min linear gradient to 57% solvent B (acetonitrile:methanol:water, 45:45:10 v/v), 4 min of 100% solvent B, followed by a 5 min linear gradient to 100% solvent A. The flow rate was 2 mL min^{-1}. Primary AA were detected with a fluorescence detector (FLD-3400 RS; Thermo Scientific) at 340 and 450 nm (excitation and emission fluorescence), while secondary AA (i.e., proline) were detected with the UV detector reported above at 262 nm. To quantify the content of AA, known amounts of pure authentic standards were injected into the UHPLC system and equations, correlating peak area to AA concentration, were formulated using the software reported above. Data are shown as nonaromatic AA (sum of aspartic acid, asparagine, glutamic acid, glutamine, lysine, threonine, leucine, isoleucine, valine, alanine, arginine, glycine, and histidine), aromatic AA (sum of tyrosine, tryptophan, and phenylalanine) and AA with special functions (sum of cysteine, methionine, and proline).

Statistical analyses

The Shapiro–Wilk's and Levene's tests were used to firstly assess the normal distribution of data and the homogeneity of variance, respectively. The effect of time on AUDPC was investigated by a one-way analysis of variance (ANOVA). The effects of *V. dahliae* inoculation, time and their interaction on parameters collected with non-destructive measurements (investigating the same leaf samples at all times of analysis; i.e., A, g_s, C_i, F_v/F_m, and PI) were assessed by a one-way repeated-measures ANOVA (using '*V. dahliae* inoculation' as between factor and 'time' as within factor); while those on parameters collected with destructive measurements (investigating different leaf samples at each time of analysis; i.e., 0, 2, 4, 6, 8, 10 wpi) were assessed by a two-way ANOVA (using '*V. dahliae* inoculation' and 'time' as factors). Comparison among means were determined by the Tukey's HSD post-hoc test. Effects with $P \leq 0.05$ were considered statistically significant. Statistical analyses were performed with JMP 11.0 (SAS Institute, Cary, NC, USA).

Results

Verticillium re-isolation, and disease severity progress

Verticillium was successfully re-isolated from inoculated plants after 5 wpi, as confirmed by the identification of typical *Verticillium* conidiophores, conidia and melanized microsclerotia. Infected plants progressively showed (i) marginal chlorosis of leaflets already at 2 wpi, which progressively spread on the entire leaf surface, (ii) yellowing symptoms that developed in wilting at around 6 wpi, (iii) a gradually falling of both leaflets and leaves at about 8 wpi, and (iv) a final severe defoliation at the end of the experiment (Fig. 2a). As a consequence, AUDPC values significantly increased at each time of analysis ($P \leq 0.001$), reaching a maximum value at 10 wpi (Fig. 2b).

Ecophysiological responses and water status

Table 1 shows the effects (i.e., *P* levels) of *V. dahliae* inoculation, time and their interaction on both ecophysiological and water status parameters, which were always significant, except for Ψ_π. *V. dahliae* infection induced a strong reduction of A and g_s from 4 wpi (−38 and −46% in comparison with controls,

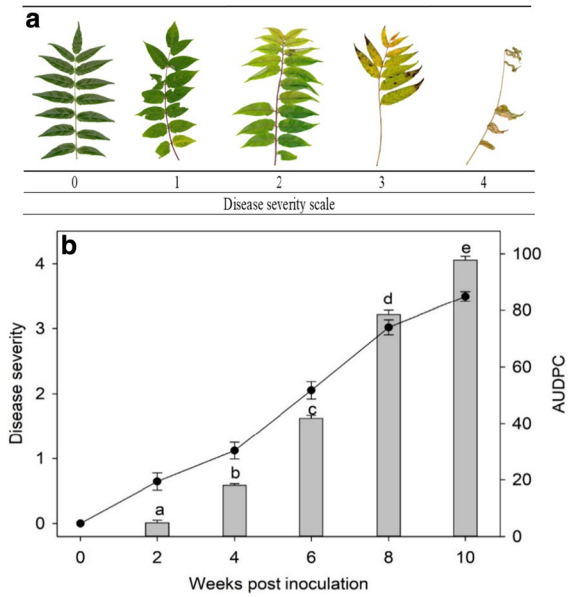

Fig. 2 **a** Disease severity scale rated according to the percentage of damage of affected leaves: 0 = no symptoms; 1 = 1–33%; 2 = 34–66%; 3 = 67–99%; 4 = dead leaf. **b** Disease severity progress (line/scatter plot) and Area Under the Disease Progress Curve (AUDPC, bar plot) assessed on *Ailanthus altissima* plants at 0, 2, 4, 6, 8 and 10 weeks post inoculation with *Verticillium dahliae*. Data are shown as mean ± standard error (n = 20). Different letters indicate significant differences among AUDPC means, according to the Tukey's HSD post hoc test ($P \leq 0.05$)

respectively) until the end of the experiment (Fig. 3a, b). C_i levels resulted higher in control plants at 4 wpi (+ 10% compared with *V. dahliae*-inoculated ones), whereas they were higher in *V. dahliae*-inoculated plants at the following times of analysis (+ 8%, as average), reaching a maximum at the end of the experiment (Fig. 3c). *Verticillium dahliae*-inoculated plants showed lower V_{cmax} values than controls (− 16%) at 6 wpi, whereas no significant differences were observed at 10 wpi. Conversely, J_{1500} values strongly decreased in *V. dahliae*-inoculated plants only at the end of the experiment (− 40%; Table 2).

Verticillium dahliae infection induced a strong reduction of PI_{ABS} values from 4 wpi (− 77%, compared with controls) until the end of the experiment, when the minimum PI_{ABS} level was reached (Fig. 4a). A significant *V. dahliae*—induced reduction of F_v/F_m was instead observed from 6 wpi (− 30%), but again reaching the minimum value at 10 wpi (Fig. 4b). Fast fluorescence kinetics confirmed a decreasing trend of photosynthetic performances determined by *V. dahliae* inoculation (particularly evident from 8 wpi), as reflected by the flattening of transient curves. On the other hand, transient curves of control plants maintained a typical profile of healthy samples (Fig. 4c).

Both Ψ_{LW} and RWC were significantly reduced by *V. dahliae* inoculation from 4 wpi (− 24 and − 14% compared with controls, respectively) until the end of the experiment, reaching minimum values at 10 and 6 wpi, respectively (2.1 ± 0.1 and 64 ± 1; Fig. 5a, b). Inoculation, time and their interaction did not affect $\Psi_{L\pi}$.

Biochemical responses

Table 1 also shows the effects (i.e., *P* levels) of *V. dahliae* inoculation, time and their interaction on biochemical parameters, which were always significant, except for the effect of time on Tot starch and of *V. dahliae* inoculation on nonaromatic and aromatic AA. *V. dahliae* inoculation induced a significant reduction of K^+/Na^+ ratio from 6 wpi (fourfold lower than controls), as well as of both K^+/Mg^{2+} and K^+/Ca^{2+} ratios from 8 wpi (− 80 and − 87%, respectively), and these trends were maintained until the end of the experiment. Specifically, these ratios significantly increased at the latest analysis times only in control plants (Fig. 6).

Verticillium dahliae inoculation induced a strong decrease of Chl tot from 2 wpi (-44% compared with controls; Fig. 7a), whereas it trigged an accumulation of zeaxanthin (Zea) from 4 wpi (+ 30%; Fig. 7b), and these trends lasted until the end of the experiment. Similarly, a huge increase of ABA was observed in infected plants from 8 wpi (about threefold higher than controls; Fig. 7c). Both Zea and ABA contents reached maximum values at 10 wpi.

A significant *V. dahliae*-induced decrease of Tot car occurred from 2 wpi (− 34% compared with controls) until the end of the experiment (except at 4 wpi), reaching the minimum at 6 wpi (Fig. 8a). Conversely, the effects of *V. dahliae* inoculation on starch content was not stable throughout the experiment: starch content was reduced at 2 and 4 wpi (− 16 and − 30%, respectively), showed no differences between experimental groups at 6 and 8 wpi, and finally increased at the end of the experiment (+ 86%; Fig. 8b).

Table 1 *P* levels (***$P \leq 0.001$, **$P \leq 0.01$; *$P \leq 0.05$; ns $P > 0.05$) and degrees of freedom (d.f) of one-way ANOVA for the effects of *Verticillium dahliae* inoculation, time, and their interaction on photosynthetic rate (A), stomatal conductance (g_s), intercellular CO_2 concentration (C_i), photosynthetic performance index (PI_{ABS}), and potential PSII photochemical activity (F_v/F_m ratio), assessed by a one-way repeated measures ANOVA (using 'Vd inoculation' as between factor and 'time' as within factor); and on leaf water potential (Ψ_{LW}), relative water content (RWC), leaf osmotic potential ($\Psi_{L\pi}$), K^+/Na^+, K^+/Ca^{2+}, K^+/Mg^{2+} ratio, total chlorophylls (Chl tot), zeaxanthin (Zea), abscisic acid (ABA), total carbohydrates (Tot car), starch (starch), nonaromatic amino acids (AA nonaromatic), aromatic amino acids (AA aromatic) and amino acids with special functions (AA special function), assessed by a two-way ANOVA (using '*V. dahliae* inoculation' and 'time' as factors)

	d.f	Inoculation	d.f	Time	d.f	Inoculation × Time
A	1	***	5	***	5	***
g_s	1	***	5	***	5	***
C_i	1	***	5	*	5	***
PI_{ABS}	1	**	4	***	4	***
F_v/F_m	1	***	4	**	4	**
Ψ_{LW}	1	***	5	**	5	***
Ψ_{π}	1	ns	5	ns	5	ns
RWC	1	***	5	***	5	**
K^+/Na^+	1	**	5	***	5	***
K^+/Ca^{2+}	1	**	5	***	5	***
K^+/Mg^{2+}	1	***	5	***	5	***
Chl tot	1	***	5	***	5	**
Zea	1	***	5	***	5	***
ABA	1	***	5	***	5	***
Tot car	1	***	5	***	5	***
Tot starch	1	***	5	ns	5	***
AA nonaromatic	1	ns	5	***	5	***
AA aromatic	1	ns	5	***	5	***
AA special function	1	***	5	***	5	***

Verticillium dahliae inoculation avoided the accumulation of nonaromatic AA which was instead observed in control plants at 4 wpi (nonaromatic AA were 68% lower in inoculated plants than in controls), whereas it significantly increased the content of these compounds at 6 wpi (twofold higher than controls), and no differences were reported at the other times of analysis (Fig. 9a). Among nonaromatic AA, aspartic acid, glutamic acid and lysine were the most abundant in all samples (*data not shown*). A remarkable peak of aromatic AA content was induced by *V. dahliae* inoculation at 8 wpi (sixfold higher than controls; Fig. 9b), while no differences between experimental groups were observed at the other times of analysis. Among aromatic AA, phenylalanine was the most abundant in all samples (*data not shown*). *Verticillium dahliae* inoculation also increased the content of AA with special function at 4 wpi, and even more at 8 wpi (4- and 10- fold higher than controls, respectively; Fig. 9c), but also these compounds did not show other significant differences at the other times of analysis. Among AA with special function, proline was the most abundant in all samples (*data not shown*).

Discussion

Plants introduced into a new geographic region may encounter other multiple pathogens with different infection strategies compared to those occurring in their native areas (Schall and Davis 2009b). This is the case of the tree-of heaven affected by Verticillium wilt: although *Verticillium* spp. are not mentioned among *Ailanthus* enemies in the native areas of the tree species, they have been reported as primary pathogens causing *Ailanthus* decay and extensive mortality in other worldwide regions severely challenged by this invasive species (Ding et al. 2006). Verticillium

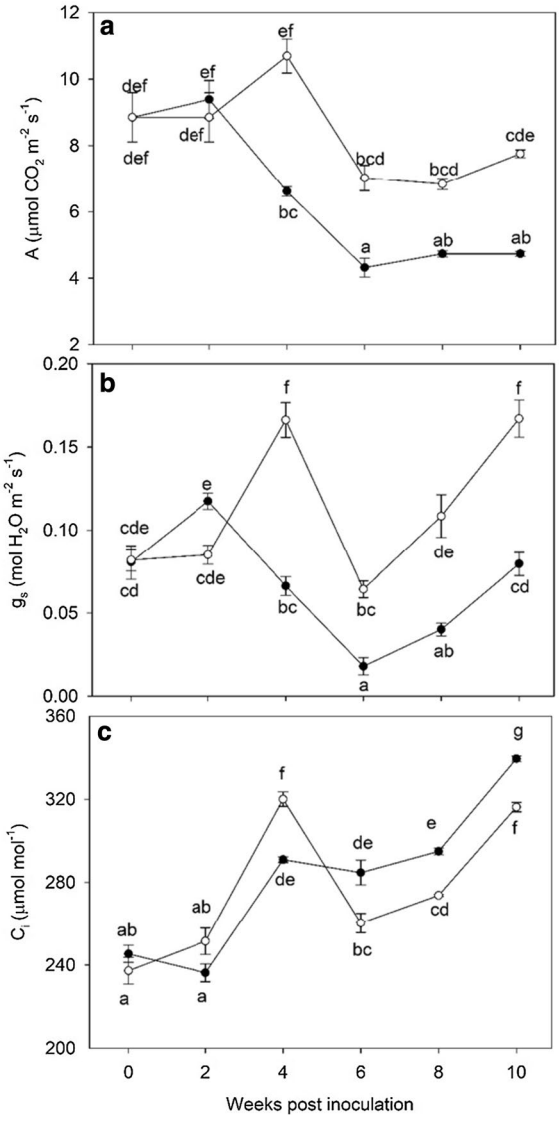

Fig. 3 Net CO_2 assimilation rate (A, **a**); stomatal conductance (g_s, **b**) and intercellular CO_2 concentration (C_i, **c**) in *Ailanthus altissima* plants inoculated with *Verticillium dahliae* (black circle) or not inoculated (controls, white circle). Measurements were carried out at 0, 2, 4, 6, 8 and 10 weeks post inoculation. Data are shown as mean ± standard error (n = 5). Since the one-way repeated measures ANOVA revealed a significant *V. dahliae* inoculation × time interaction on these parameters, different letters indicate significant differences among means, according to the Tukey's HSD post hoc test ($P \leq 0.05$)

wilt of *Ailanthus* appeared sporadically in the past, although cases of *Ailanthus* mortality have been well documented since long, especially in urban areas (Kasson et al. 2014; Pisuttu et al. 2020a). Probably,

Table 2 Maximum rate of carboxylation of Rubisco (V_{cmax} μmol CO_2 m^{-2} s^{-1}) and electron transport obtained at saturating light (J_{1500} μmol e^- m^{-2} s^{-1}) in leaves of *Ailanthus altissima* plants uninoculated (control) or stem-inoculated with *Verticillium dahliae* (Vd-inoculated), analysed at 6 and 10 weeks post inoculation (wpi)

Time	Inoculation	V_{cmax}	J_{1500}
6 wpi	Control	54 ± 1	49 ± 1
	Vd-inoculated	46 ± 1	43 ± 3
		**	ns
10 wpi	Control	213 ± 10	227 ± 24
	Vd-inoculated	186 ± 1	136 ± 22
		ns	*

Data are shown as mean ± standard error (n = 3). For each time and each parameter, *P*-values are from Student's t test for the effects of inoculation: $^{**}P \leq 0.01$, $^{*}P \leq 0.05$, ns: $P > 0.05$

Verticillium wilt of *Ailanthus*, as well as cases of high natural mortality rates of *Ailanthus* within urban or peri-urban sites, were neglected and confused for years. Many Verticillium wilt epidemics were likely overlooked, mistaken for natural senescence and explained as short life expectancy of *Ailanthus*, or even interpreted as the result of chemical applications along roadsides (Kasson et al. 2014). Considering the incomplete understanding of this plant-pathogen interaction, information regarding the physiological and biochemical responses of the invasive species trying to cope with the wilt pathogen was lacking, a gap addressed by the present study.

Verticillium diseases are not easy to diagnose in nature because of the absence of pathognomonic symptoms (Fradin and Thomma 2006) and also in this experiment the development of visible injuries, as well as changes in other parameters (mostly at 4 wpi), did not occur simultaneously to the pathogen re-isolation (at 5 wpi). Curiously, sometimes wilting symptoms are not shown in plants affected by Verticillium wilt. This is not the case of the present study, since inoculated *Ailanthus* plants progressively showed marginal chlorosis (also Chl tot decreased since 2 wpi), yellowing and indeed wilting, before starting to fall leaflets and leaves, until a final severe defoliation; so confirming the high virulence of the *V. dahliae*—strain VdGL16. The main reason for the occurrence of these Verticillium wilt symptoms is usually the occlusion of xylem vessels due to (i) physical blockage by the pathogen itself and (ii) host

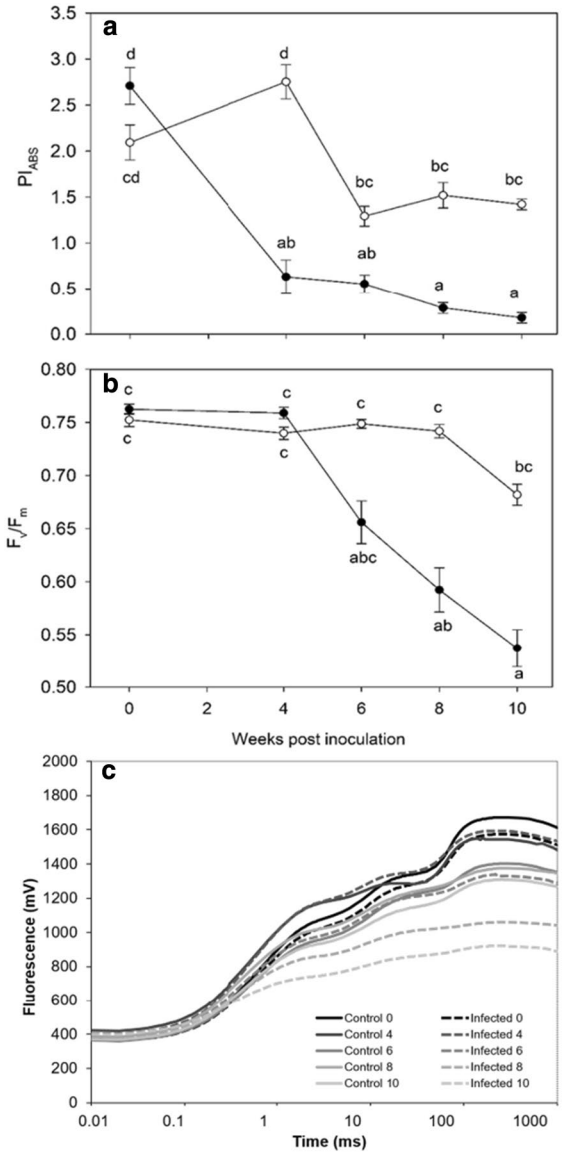

Fig. 4 Photosynthetic Performance Index (PI_{ABS}, **a**) and maximum of quantum yield of primary photochemistry (F_v/F_m, **b**) in *Ailanthus altissima* plants inoculated with *Verticillium dahliae* (black circle) or not inoculated (controls, white circle). Measurements were carried out analysed at 0, 4, 6, 8 and 10 weeks post inoculation. Data are shown as mean ± standard error (n = 5). Since the one-way repeated measures ANOVA revealed a significant *V. dahliae* inoculation × time interaction on these parameters, different letters indicate significant differences among means according to the Tukey's HSD post hoc test ($P \leq 0.05$). Average fast fluorescence transient curves of infected and control plants at 0, 4, 6, 8 and 10 weeks post inoculation, plotted on logarithmic scale (**c**)

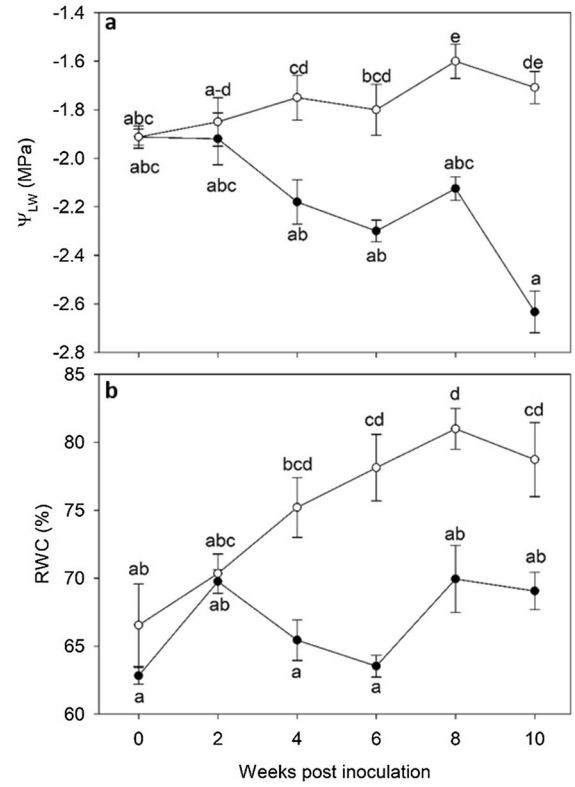

Fig. 5 Leaf water potential (Ψ_{LW}, **a**) and relative water content (RWC, **b**) in *Ailanthus altissima* plants inoculated with *Verticillium dahliae* (black circle) or not inoculated (controls, white circle). Measurements were carried out at 0, 2, 4, 6, 8 and 10 weeks post inoculation. Data are shown as mean ± standard error (n = 5). Since the two-way ANOVA revealed a significant *V. dahliae* inoculation × time interaction on these parameters, different letters indicate significant differences among means, according to the Tukey's HSD post hoc test ($P \leq 0.05$)

defence responses that are aimed at vessel plugging, such as production of tyloses and gums (Fradin and Thomma 2006), which basically cause a water stress. It is known that the growth and activity of *V. dahliae* may trigger plant physiological responses that resemble those commonly caused by drought (such as reduction in leaf photosynthesis, transpiration and leaf longevity; Lorenzini et al. 1997; Sadras et al. 2000; Pascual et al. 2010). Although *Ailanthus* is considered as drought-tolerant (Filippou et al. 2014) thanks to its ability to reduce both water loss by leaves and root hydraulic conductance (Trifilò et al. 2003), the fungal infection rapidly and severely compromised the plant water status (as confirmed by the reduced RWC and Ψ_{LW} values from 4 wpi), likely

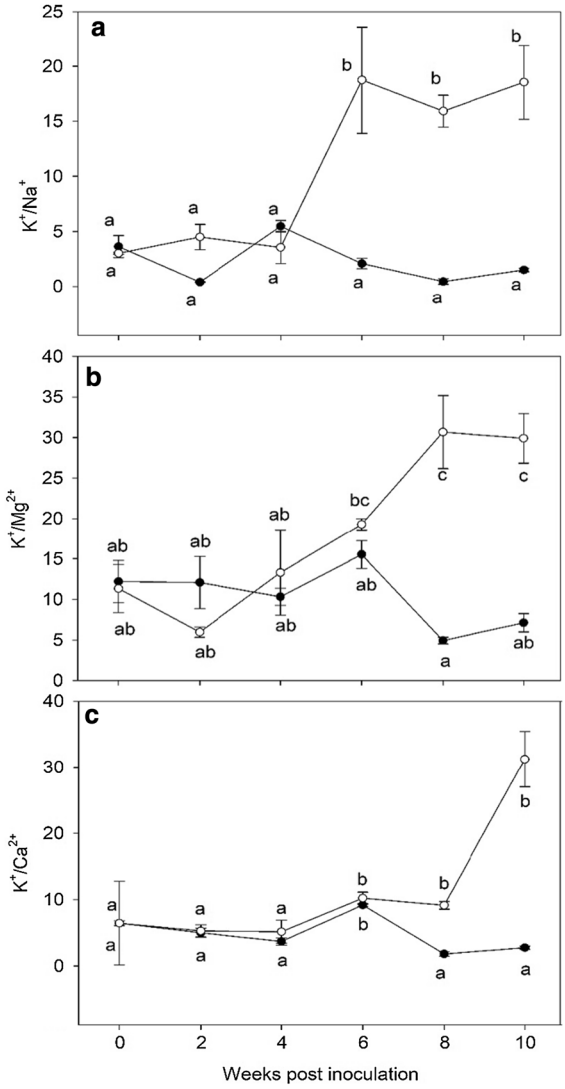

Fig. 6 K^+/Na^+ (**a**), K^+/Mg^{2+} (**b**) and K^+/Ca^{2+} ratios (**c**) in *Ailanthus altissima* plants inoculated with *Verticillium dahliae* (black circle) or not inoculated (controls, white circle). Measurements were carried out at 0, 2, 4, 6, 8 and 10 weeks post inoculation. Data are shown as mean ± standard error (n = 3). Since the two-way ANOVA revealed a significant *V. dahliae* inoculation × time interaction on these parameters, different letters indicate significant differences among means according to the Tukey's HSD post hoc test ($P \leq 0.05$)

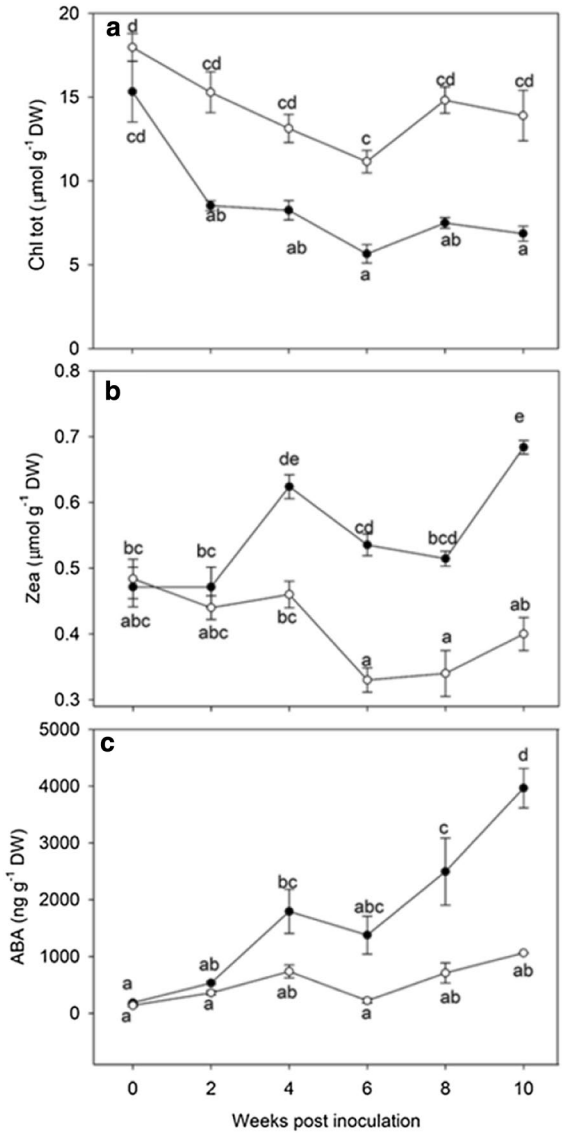

Fig. 7 Total chlorophyll (Chl tot, **a**), zeaxanthin (Zea, **b**) and abscisic acid (ABA, **c**) contents in *Ailanthus altissima* plants inoculated with *Verticillium dahliae* (black circle) or not inoculated (controls, white circle). Measurements were carried out at 0, 2, 4, 6, 8 and 10 weeks post inoculation. Data are shown as mean ± standard error (n = 3), on a dry weight (DW) basis. Since the two-way ANOVA revealed a significant *V. dahliae* inoculation × time interaction on these parameters, different letters indicate significant differences among means according to the Tukey's HSD post hoc test ($P \leq 0.05$)

due to a vascular dysfunction. Moreover, *Verticillium* produces a broad spectrum of phytotoxins and other molecules inducing host cell death that also play a crucial role in the pathogenicity of the organism (Fradin and Thomma 2006). Actually, the mechanistic basis of disease-induced inhibition of photosynthetic performance in *Verticillium* wilted plants remains unclear to date and the decay could probably due by both, the *V. dahliae*-induced vascular dysfunction and the production of phytotoxins. In fact, if in

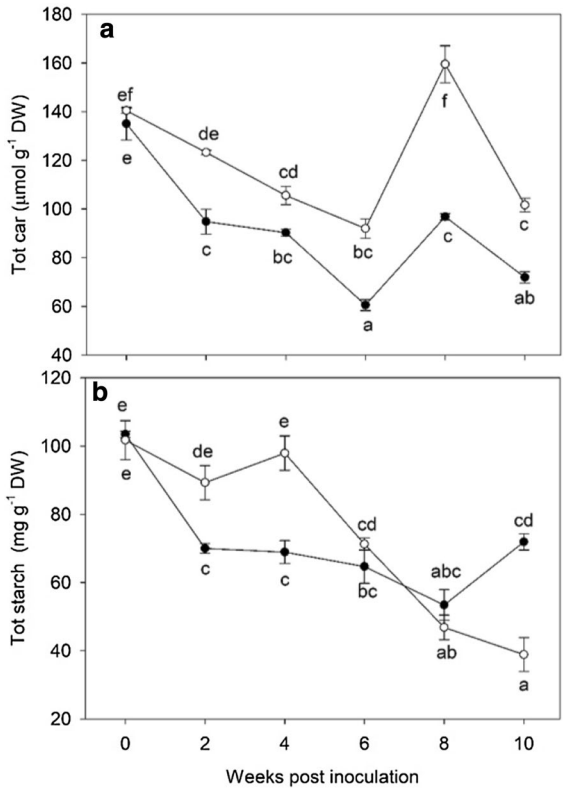

Fig. 8 Total carbohydrates (Tot car, **a**) and Total starch (Tot Starch, **b**) contents in *Ailanthus altissima* plants inoculated with *Verticillium dahliae* (black circle) or not inoculated (controls, white circle). Measurements were carried out at 0, 2, 4, 6, 8 and 10 weeks post inoculation. Data are shown as mean ± standard error (n = 3), on a dry weight (DW) basis. Since the two-way ANOVA revealed a significant *V. dahliae* inoculation × time interaction on these parameters, different letters indicate significant differences among means according to the Tukey's HSD post hoc test ($P \leq 0.05$)

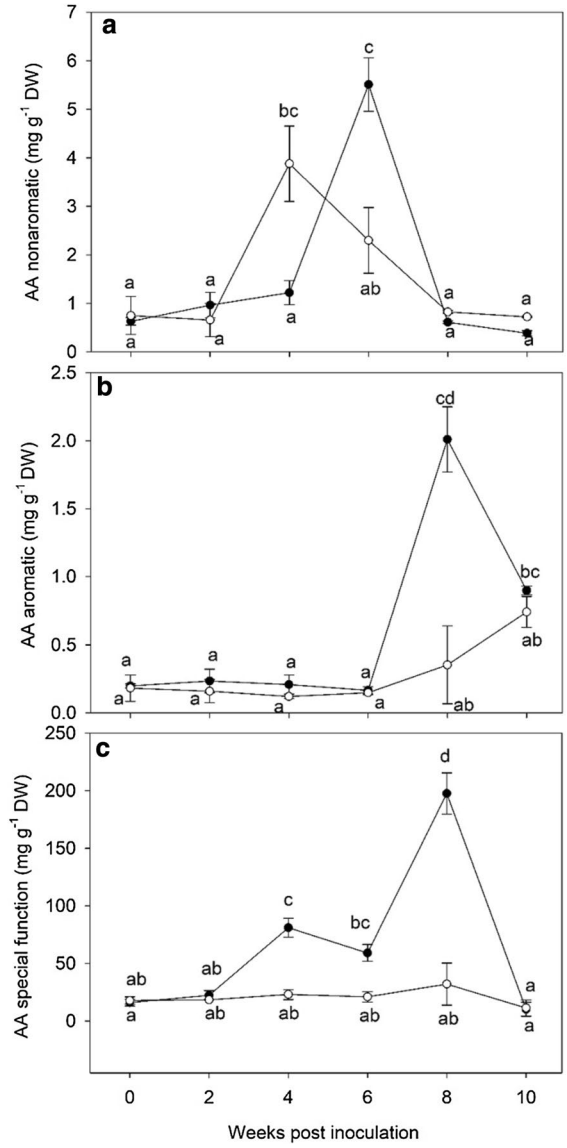

Fig. 9 Nonaromatic amino acids (AA nonaromatic, **a**), aromatic amino acids (AA aromatic, **b**) and amino acids with special function (AA special function, **c**) contents in *Ailanthus altissima* plants inoculated with *Verticillium dahliae* (black circle) or not inoculated (controls, white circle). Measurements were carried out at 0, 2, 4, 6, 8 and 10 weeks post inoculation. Data are shown as mean ± standard error (n = 3), on a dry weight (DW) basis. Since the two-way ANOVA revealed a significant *V. dahliae* inoculation × time interaction on these parameters, different letters indicate significant differences among means according to the Tukey's HSD post hoc test ($P \leq 0.05$)

plants grown in harsh conditions, stomatal closure can be considered one of the initial responses in order to retain water and provide innate immunity against pathogens (Bharath et al. 2021), here photosynthesis was impaired (already from 4 wpi) due to both stomatal and mesophyll limitations (as confirmed by the reduced g_s and the concomitant increased C_i), suggesting the role of other pathogenic mechanisms apart from water stress (Nogués et al. 2002), and followed by biochemical impairments in terms of Rubisco carboxylation efficiency at 6 wpi and regeneration capacity at the end of the experiment (decreased V_{cmax} and J_{1500} values, respectively).

The detrimental effects of *V. dahliae* inoculation on photosynthetic system was further confirmed by variations of Chl *a* fluorescence parameters. In particular, the reduction of PI_{ABS} (already from 4 wpi, concomitantly with A decline) and F_v/F_m ratio, together with the overall alteration of Chl *a* fluorescence emission curves suggested that the disease (i) compromised the photosynthetic activity of the PSII RC complex (Strasser et al. 2000), (ii) induced the closure of a large proportion of PSII reaction centres, and (iii) caused a progressively increasing photoinhibition (Lorenzini et al. 1997; Nogués et al. 2002; Pisuttu et al 2020b). Consequently, the light energy used in photochemistry exceeded the electron transport capacity to $NADP^+$ and the decreased ΔpH across the thylakoid membranes promoted the oxidative cleavage of the carotenoids, which can lead to the production of ABA (Pisuttu et al. 2020b). This hypothesis was also confirmed by the significant increase in Zea content observed from 4 wpi, since it is known that Zea can be used to de novo synthesize ABA (Zhou et al. 2015). This hormone usually plays a pivotal role in the physiological adaptation of plants under environmental constraints, especially by regulating stomatal opening, and so controlling transpiration and water loss (Mauch Mani and Mauch 2005; Munemasa et al. 2015). However, the involvement of ABA in disease susceptibility has been shown to be complex and dependent on multiple factors such as the type of pathogen and the duration of infection (Asselbergh et al. 2008). In particular, ABA accumulation during the early stages of pathogen infection commonly increases plant resistance (e.g., by stomatal closure, callose production and enhancement of jasmonic acid response), while at later invasion stages it makes plants more susceptible by repressing mechanisms involved in disease resistance (e.g., additional callose accumulation, phenylpropanoid and lignin biosynthesis; Maksimov 2009). Here, a significant increase of ABA content was only observed from 8 wpi suggesting that it likely obstructed the activation of defence mechanisms by promoting early leaf senescence and nutrient remobilization (Schmidt et al. 2008; Saddhe et al. 2017).

In the current experiment, *V. dahliae* infection also altered the ion regulations (as confirmed by the lowered K^+/Na^+, K^+/Mg^{2+} and K^+/Ca^{2+} ratios occurred from 6/8 wpi). This phenomenon could be due to (i) no ionic replacement, (ii) occlusion of vascular traits making impossible the nutrient translocation from roots to shoots, and/or (iii) utilization of mineral elements for other functions such as osmolyte accumulation, hypersensitive response and programmed cell death (Lecourieux et al. 2002, Amtmann et al. 2008, Ranf et al. 2011, Wang and Wu 2013). In particular, the osmotic potential did not change compared with controls and only proline (the most relevant compound among AA with special function) markedly accumulated at 8 wpi (Filippou et al. 2014; Tani et al. 2018). Proline has multiple positive roles in stress adaptation, recovery, and signalling as a response to a wide range of biotic and abiotic stresses. It is involved not only in intracellular osmotic adjustment between cytoplasm and vacuole, but also in regulation of plant growth and protection of chloroplasts (Bibi et al. 2014). Consequently, some authors considered proline accumulation as a sensor of wilt damage caused by *V. dahliae* (Goicoechea et al. 2000). Here, the observed shift of osmolyte accumulations might be a direct effect of *V. dahliae* in view of the redistribution of solutes in plant cells and the blockage of micro- and macronutrient translocation (as confirmed by the significant decrease of Tot car; Liang et al. 2013). In general, it could be supposed that primary metabolism in *V. dahliae* inoculated plants is strongly delayed by the disease as confirmed also by the profile of nonaromatic AA, that showed a huge increase at 4 wpi in controls while only 2 weeks later in infected trees (without substantial qualitative changes). Moreover, our results indicated that the occlusion of vascular traits interfered with the sugar transport through the conducting elements. Since sugars homeostasis is a dynamic process in which starch and sucrose undergo interconversion as needed by the cells (Thalmann and Santelia 2017), a huge consumption of simple sugars and starch reserves likely occurred without replacement of new photosynthesized (according to the decay of the photosynthetic performances). These compounds - being the primary carbon and energy source in plants - produce reducing power for the biosynthesis of non-enzymatic antioxidants such as glutathione, ascorbate and phenolic compounds (in accordance with the increase of phenylalanine among aromatic AA) that could (i) limit the generation of ROS (Novo et al. 2017), (ii) inhibit pathogen growth, and (iii) act as antimicrobial and cell wall strengthener (e.g., suberin;

Jabeen et al. 2009; Shaban et al. 2018). Effectively, the increase of aromatic AA at 8 wpi, mainly due by phenylalanine, could be considered an attempt of response against *Verticillium* infection, since this AA represents the common precursor of phenylpropanoids (Eich 2008). However, considering that plants were strongly affected by the fungal infection, further investigations are needed to elucidate the potential role of secondary metabolism in the *Ailanthus*/*V. dahliae* interaction, even if triggered in a late-stage of plant disease.

In conclusion, our results reflect the susceptibility of *A. altissima* to *V. dahliae* in terms of visible injury, alteration of the photosynthetic apparatus, and hydric status. However, the onset of water stress did not set-in motion the series of physiological events and osmotic adjustments analogous to those occurring in drought-resistant plants, and *V. dahliae*-infected plants were not able to delay senescence and defoliation (already observed at the end of August), so suggesting to further investigate the production of phytotoxic compounds which likely played a crucial role in *V. dahliae* pathogenicity. Furthermore, in the optic of ecological behaviour of *Ailanthus* in non-endemic ecosystems, it would be important to understand (i) the role(s) played by phytohormones in *Ailanthus* responses to *V. dahliae* (defence or resistance) and (ii) at what rate the *V. dahliae* infection limits the production of phenolic compounds and allelopathic substances that characterize *Ailanthus* invasiveness. Nevertheless, the potential use of *V. dahliae* as biological control agent requests accuracy in the distribution (safe procedure of application) and tests in open field, constantly assessing all potential risk factors, considering that (i) artificial inoculations in controlled environments (e.g., laboratories and greenhouses) are commonly optimal for pathogen growth, and (ii) plant susceptibility does not necessarily indicate that symptomatic species would be "natural hosts" under suboptimal or optimal field conditions, or within a heterogeneous landscape (Barton 2004). This suggests to firstly test *V. dahliae* in protected field conditions, then in urban and peri-urban areas in which the presence of potential hosts is limited, as well as in monumental sites, and finally to collect evidences also in different ecosystems. Overall, the present study highlights the aggressiveness of *Verticillium* spp. towards *Ailanthus* and according to previous works (Schall and Davis 2009a, b; Maschek and Halmschlager 2018; Brooks et al. 2020), it confirms that *Verticillium* spp. can be considered the only endemic natural enemy able to quickly compromise the physiochemical activity of affected *Ailanthus*, causing inevitably the decline of the invasive tree species so far.

Acknowledgements We thank Dr. Mariagrazia Tonelli, Dr. Ferruccio Filippi and Ms Simona Ciangherotti for helping in lab analyses and plant management before and during the experimental procedures.

Author contributions Conceptualization, EP, CN, GL; methodology, CP; ELP and LP; formal analysis, CP; ELP and LP; data curation, CP; ELP and LP writing-original draft preparation, CP, EP; writing-review and editing, CP, EP, LC; supervision, GL and CN. All authors have read and agreed to the published version of the manuscript.

Funding Open access funding provided by Università di Pisa within the CRUI-CARE Agreement. The authors declare that no funds, grants, or other support were received during the preparation of this manuscript.

Declarations

Conflict of interest The authors have no relevant financial or non-financial interests to disclose.

References

Amtmann A, Troufflard S, Armengaud P (2008) The effect of potassium nutrition on pest and disease resistance in plants. Physiol Plant 133:682–691. https://doi.org/10.1111/j.1399-3054.2008.01075.x

Asselbergh B, De Vleesschauwer D, Höfte M (2008) Global switches and fine-tuning-ABA modulates plant pathogen defense. Mol Plant Microbe Interact 21:709–719. https://doi.org/10.1094/MPMI-21-6-0709

Badalamenti E, Barone E, La Mantia T (2015) Seasonal effects on mortality and resprouting of stems treated with glyphosate in the invasive tree of heaven (*Ailanthus altissima*).

Arboric J 37:180–195. https://doi.org/10.1080/03071375.2015.1112163
Barton J (2004) How good are we at predicting the field host-range of fungal pathogens used for classical biological control of weeds? Biol Control 31:99–122. https://doi.org/10.1016/j.biocontrol.2004.04.008
Bernacchi CJ, Portis AR, Nakano H, Von Caemmerer S, Long SP (2002) Temperature response of mesophyll conductance. Implications for the determination of Rubisco enzyme kinetics and for limitations to photosynthesis in vivo. Plant Physiol 130:1992–1998. https://doi.org/10.1104/pp.008250
Bharath P, Gahir S, Raghavendra AG (2021) Abscisic acid-induced stomatal closure: an important component of plant defense against abiotic and biotic stress. Front Plant Sci 12:615114. https://doi.org/10.3389/fpls.2021.615114
Bibi N, Fan K, Dawood M, Nawaz G, Yuan SN, Wang XD (2014) Exogenous application of epibrassinolide attenuated *Verticillium* wilt in upland cotton by modulating the carbohydrates metabolism, plasma membrane ATPases and intracellular osmolytes. Plant Growth Regul 73:155–164. https://doi.org/10.1007/s11356-017-8738-6
Brooks RK, Wickert KL, Baudoina A, Kasson MT, Salom S (2020) Field-inoculated *Ailanthus altissima* stands reveal the biological control potential of *Verticillium nonalfalfae* in the mid-Atlantic region of the United States. Biol Control l 148:104298. https://doi.org/10.1016/j.biocontrol.2020.104298
Calzone A, Cotrozzi L, Pellegrini E, Guidi L, Lorenzini G, Nali C (2020) Differential response strategies of pomegranate cultivars lead to similar tolerance to increasing salt concentrations. Sci Hortic 271:109441. https://doi.org/10.1016/j.scienta.2020.109441
Cotrozzi L, Pellegrini E, Guidi L, Landi M, Lorenzini G, Massai R, Remorini D, Tonelli M, Trivellini A, Vernieri P, Nali C (2017) Losing the warning signal: drought compromises the cross-talk of signaling molecules in *Quercus ilex* exposed to ozone. Front Plant Sci 8:1020. https://doi.org/10.3389/fpls.2017.01020
Cotrozzi L, Peron R, Tuinstra MR, Mickelbart MV, Couture JJ (2020) Spectral phenotyping of physiological and anatomical leaf traits related with maize water status. Plant Physiol 184:1363–1377. https://doi.org/10.1104/pp.20.00577
De Feo V, De Martino L, Quaranta E, Pizza C (2003) Isolation of phytotoxic compounds from tree-of-heaven (*Ailanthus altissima* Swingle). J Agr Food Chem 26:1177–1180. https://doi.org/10.1002/ptr.1670
Ding J, Wu Y, Zheng H, Fu W, Reardon R, Liu M (2006) Assessing potential biological control of the invasive plant, tree-of heaven, *Ailanthus altissima*. Biocontrol Sci Technol 16:547–566. https://doi.org/10.1080/09583150500531909
DiTomaso JM, Kyser GB (2007) Control of *Ailanthus altissima* using stem herbicide application techniques. Arb Urban for 33:55–63
Eich E (2008) Solanaceae and convolvulaceae: secondary metabolites. Springer, Berlin
EPPO (2020) PM 9/29 (1) *Ailanthus altissima*. EPPO Bulletin 50:148–155. https://doi.org/10.1111/epp.12621
Farquhar GD, Von Caemmerer S, Berry JA (1980) A biochemical model of photosynthetic CO_2 assimilation in leaves of C3 species. Planta 149:78–90. https://doi.org/10.1007/BF00386231
Filippou P, Bouchagier P, Skotti E, Fotopoulos V (2014) Proline and reactive oxygen/nitrogen species metabolism is involved in the tolerant response of the invasive plant species *Ailanthus altissima* to drought and salinity. Environ Exp Bot 97:1–10. https://doi.org/10.1016/j.envexpbot.2013.09.010
Fish WW (2012) A reliable methodology for quantitative extraction of fruit and vegetable physiological amino acids and their subsequent analysis with commonly available HPLC Systems. Food Sci Nutr 3:863–871. https://doi.org/10.4236/fns.2012.36115
Fogliatto S, Ferrero A, Vidotto F (2020) Current and future scenarios of glyphosate use in Europe: are there alternatives? In: Sparks DL (ed) Advances in agronomy. Academic Press, Cambridge, pp 219–278
Fradin EF, Thomma BPHJ (2006) Physiology and molecular aspects of Verticillium wilt diseases caused by *V. dahliae* and *V. albo-atrum*. Mol Plant Pathol 7:71–86. https://doi.org/10.1111/j.1364-3703.2006.00323.x
Goicoechea N, Aguirreolea J, Cenoz S, Garcia-Mina JM (2000) *Verticillium dahliae* modifies the concentrations of proline, soluble sugars, starch, soluble protein and abscisic acid in pepper plants. Eur J Plant Pathol 106(1):19–25. https://doi.org/10.1023/A:1008724816041
Hu SY (1979) Ailanthus. Arnoldia 39:29–50
Izsépi F, Varjas V, Tóth T, Koncz L, Tenorio-Baigorria I, Végh A (2018) First report of Verticillium wilt of *Ailanthus altissima* in Hungary caused by *Verticillium dahliae*. Plant Dis 102:1454. https://doi.org/10.1094/PDIS-12-17-1914-PDN
Jabeen N, Ahmed N, Ghani MY, Sofi PV (2009) Role of phenolic compounds in resistance to chilli wilt. Commun Biometry Crop Sci 4:52–61
Kasson MT, Short DPG, O'Neal ES, Subbarao KV, Davis DD (2014) Comparative pathogenicity, biocontrol efficacy, and multilocus sequence typing of *Verticillium nonalfalfae* from the invasive *Ailanthus* and other hosts. Phytopathology 104:282–292. https://doi.org/10.1094/PHYTO-06-13-0148-R
Kasson MT, O'Neal ES, Davis DD (2015) Expanded host range testing for *Verticillium nonalfalfae*: potential biocontrol agent against the invasive *Ailanthus altissima*. Plant Dis 99:823–835
Kowarick I, Säumel I (2007) Biological flora of Central Europe: *Ailanthus altissima* (Mill.) Swingle. Perspect Plant Ecol Evol 8:207–237. https://doi.org/10.1016/j.ppees.2007.03.002
Kowarik I, Straka TM, Lehmann M, Studnitzky R, Fischer LK (2021) Between approval and disapproval: citizens' views on the invasive tree *Ailanthus altissima* and its management. NeoBiota 66:1–30. https://doi.org/10.3897/neobiota.66.63460
Lecourieux D, Mazars C, Pauly N, Ranjeva R, Pugin A (2002) Analysis and effects of cytosolic free calcium increases in response to elicitors in *Nicotiana plumbaginifolia* cells. Plant Cell 14:2627–2641. https://doi.org/10.1105/tpc.005579

Liang X, Zhang L, Natarajan SK, Becker DF (2013) Proline mechanisms of stress survival. Antioxid Redox Signal 9:998–1011. https://doi.org/10.1089/ars.2012.5074

Long SP, Bernacchi CJ (2003) Gas exchange measurements, what can they tell us about the underlying limitations to photosynthesis? Procedures and sources of error. J Exp Bot 54:2393–2401. https://doi.org/10.1093/jxb/erg262

Longa CMO, Pietrogiovanna M, Minerbi S, Andriolo A, Tolotti G, Maresi G (2019) First observation of Verticillium wilt on *Ailanthus altissima* in the Eastern Italian Alps (Trentino-South Tyrol). Plant Pathol J 101:757. https://doi.org/10.1007/s42161-018-00217-y

Lorenzini G, Guidi L, Nali C, Ciompi S, Soldatini GF (1997) Photosynthetic response of tomato plants to vascular wilt diseases. Plant Sci 124:143–152. https://doi.org/10.1016/S0168-9452(97)04600-1

Maksimov IV (2009) Abscisic acid in the plants-pathogen interaction. Russ J Plant Physiol 56:742

Mani-Mauch B, Mauch F (2005) The role of abscisic acid in plant–pathogen interactions. Curr Opin Plant Biol 8(4):409–414. https://doi.org/10.1016/j.pbi.2005.05.015

Maschek O, Halmschlager E (2017) Natural distribution of Verticillium wilt on invasive *Ailanthus altissima* in eastern Austria and its potential for biocontrol. For Pathol 47:e12356. https://doi.org/10.1111/efp.12356

Maschek O, Halmschlager E (2018) Effects of *Verticillium nonalfalfae* on *Ailanthus altissima* and associated indigenous and invasive tree species in eastern Austria. Eur J for Res 137:197–209. https://doi.org/10.1007/s10342-018-1099-y

Montecchiari S, Tesei G, Allegrezza M (2020) *Ailanthus altissima* forests determine a shift in herbaceous layer richness: a paired comparison with hardwood native forests in sub-Mediterranean Europe. Plants 9:1404. https://doi.org/10.3390/plants9101404

Moragrega C, Carol J, Bisbe E, Fabregas E, Llorente I (2021) First report of Verticillium wilt and mortality of Ailanthus altissima caused by *Verticillium dahliae* and *V. alboatrum sensu lato* in Spain. Plant Dis. https://doi.org/10.1094/PDIS-03-21-0463-PDN

Mulero-Aparicio A, Varo A, Agustí-Brisach C, López-Escudero FJ, Trapero A (2020) Biological control of Verticillium wilt of olive in the field. Crop Prot 128:104993. https://doi.org/10.1016/j.cropro.2019.104993

Munemasa S, Hauser F, Park J, Waadt R, Brandt B, Schroeder JI (2015) Mechanisms of abscisic acid-mediated control of stomatal aperture. Curr Opin Plant Biol 28:154–162. https://doi.org/10.1016/j.pbi.2015.10.010

Nentwig W, Bacher S, Kumschick S, Pysek P, Vilà M (2018) More than "100 worst" alien species in Europe. Biol Invasion 20:1611–1621. https://doi.org/10.1007/s10530-017-1651-6

Nogués S, Cotxarrera L, Alegre L, Trillas MI (2002) Limitations to photosynthesis in tomato leaves induced by *Fusarium* wilt. New Phytol 154:461–470. https://doi.org/10.1046/j.1469-8137.2002.00379.x

Novo M, Silvar C, Merino F, Martínez-Cortés T, Lu F, Ralph J, Pomar F (2017) Deciphering the role of the phenylpropanoid metabolism in the tolerance of *Capsicum annuum* L. to *Verticillium dahliae* Kleb. Plant Sci 258:12–20. https://doi.org/10.1016/j.plantsci.2017.01.014

O'Neal ES, Davis DD (2015) Biocontrol of *Ailanthus altissima*: inoculation protocol and risk assessment for *Verticillium nonalfalfae* (Plectosphaerellaceae: Phyllochorales). Biocontrol Sci Technol 25:950–969. https://doi.org/10.1080/09583157.2015.1023258

Pascual I, Azcona I, Morales F, Aguirreolea J, Sánchez Díaz M (2010) Photosynthetic response of pepper plants to wilt induced by *Verticillium dahliae* and soil water deficit. J Plant Physiol 167:701–708. https://doi.org/10.1016/j.jplph.2009.12.012

Pegg GF, Brady BL (2002) Verticillium wilts. CABI publishing, Wallingford, pp 552

Pellegrini E, Campanella A, Paolocci M, Trivellini A, Gennai C, Muganu M, Nali C, Lorenzini G (2015) Functional leaf traits and diurnal dynamics of photosynthetic parameters predict the behavior of grapevine varieties towards ozone. PLoS ONE. https://doi.org/10.1371/journal.pone.0135056

Pisuttu C, Marchica A, Bernardi R, Calzone A, Cotrozzi L, Nali C, Pellegrini E, Lorenzini G (2020a) *Verticillium wilt* of *Ailanthus altissima* in Italy caused by *V. dahliae*: new outbreaks from Tuscany. iForest 13:238–245. https://doi.org/10.3832/ifor3238-013

Pisuttu C, Pellegrini E, Cotrozzi L, Nali C, Lorenzini G (2020b) Ecophysiological and biochemical events associated with the challenge of *Verticillium dahliae* to eggplant. Eur J Plant Pathol 158:879–894. https://doi.org/10.1007/s10658-020-02122-6

Prieto P, Navarro-Raya C, Valverde-Corredor A, Amyotte SG, Dobinson KF, Mercado-Blanco J (2009) Colonization process of olive tissues by *Verticillium dahliae* and its in planta interaction with the biocontrol root endophyte *Pseudomonas fluorescens* PICF7. Microb Biotechnol 2:499–511. https://doi.org/10.1111/j.1751-7915.2009.00105.x

Ranf S, Eschen-Lippold L, Pecher P, Lee J, Scheel D (2011) Interplay between calcium signalling and early signalling elements during defence responses to microbe- or damage-associated molecular patterns. Plant J 68:100–113. https://doi.org/10.1111/j.1365-313X.2011.04671.x

Rebbeck J, Malone MA, Short DPG, Kasson MT, O'Neal ES, Davis DD (2013) First report of Verticillium wilt caused by *Verticillium nonalfalfae* on tree-of-heaven (*Ailanthus altissima*) in Ohio. Plant Dis 97:999. https://doi.org/10.1094/PDIS-01-13-0062-PDN

RKnüsel S, Conedera M, Rigling A, Fonti P, Wunder J (2015) A tree-ring perspective on the invasion of *Ailanthus altissima* in protection forests. For Ecol Manag 354:334–343. https://doi.org/10.1016/j.foreco.2015.05.010

Saddhe AA, Kundan K, Padmanabh D (2017) Mechanism of ABA signaling in response to abiotic stress in plants. In: Pandey GK (ed) Mechanism of plant hormone signaling under stress, II. Wiley, Hoboken, pp 173–195

Sadras VO, Quiroz F, Echarte L, Escande A, Pereyra VR (2000) Effect of *Verticillium dahliae* on photosynthesis, leaf expansion and senescence of field-grown sunflower. Ann Bot 86:1007–1015. https://doi.org/10.1006/anbo.2000.1267

Schall MJ, Davis DD (2009a) *Ailanthus altissima* wilt and mortality: etiology. Plant Dis 93:747–751. https://doi.org/10.1094/PDIS-93-7-0747

Schall MJ, Davis DD (2009b) Verticillium Wilt of *Ailanthus altissima*: susceptibility of associated tree species. Plant Dis 93:1158–1162. https://doi.org/10.1094/PDIS-93-11-1158

Schmidt K, Pflugmacher M, Klages S, Mäser A, Mock A, Stahl DJ (2008) Accumulation of the hormone abscisic acid (ABA) at the infection site of the fungus *Cercospora beticola* supports the role of ABA as a repressor of plant defence in sugar beet. Mol Plant Pathol 9:661–673. https://doi.org/10.1111/j.1364-3703.2008.00491.x

Shaban M, Miao Y, Ullah A, Khan AQ, Menghwar H, Khan AH, Ahmed MM, Tabassum MA, Zhu L (2018) Physiological and molecular mechanism of defence in cotton against *Verticillium dahliae*. Plant Physiol Biochem 125:193–204. https://doi.org/10.1016/j.plaphy.2018.02.011

Sheppard AW, Shaw RH, Sforza R (2006) Top 20 environmental weed for classical biological control in Europe: a review of opportunities, regulations and other barriers to adoption. Weed Res 46:93–117. https://doi.org/10.1111/j.1365-3180.2006.00497.x

Simko I, Piepho HP (2012) The area under the disease progress stairs: calculation, advantage, and application. Phytopathology 102:381–389. https://doi.org/10.1094/PHYTO-07-11-0216

Skarmoutsos G, Skarmoutsou H (1998) Occurrence of wilt disease caused by *Verticillium dahliae* on *Ailanthus glandulosa* in Greece. Plant Dis 82:129. https://doi.org/10.1094/PDIS.1998.82.1.129B

Snyder AL, Kasson MT, Salom SM, Davis DD, Griffin GJ, Kok LT (2013) First report of Verticillium wilt of *Ailanthus altissima* in Virginia caused by *Verticillium nonalfalfae*. Plant Dis 97(6):837. https://doi.org/10.1094/PDIS-05-12-0502-PDN

Stirbet A, Govindjee (2011) On the relation between the Kautsky Effect (chlorophyll *a* fluorescence induction) and Photosystem II: basics and applications of the OJIP fluorescence transient. J Photochem Photobiol B 104:236–257. https://doi.org/10.1016/j.jphotobiol.2010.12.010

Strasser RJ, Srivastava A, Tsimilli-Michael M (2000) The fluorescence transient as a tool to characterize and screen photosynthetic samples, probing photosynthesis: mechanism, regulation and adaptation. In: Yunus M, Pathre U, Mohanty P (eds) probing photosynthesis: mechanism, regulation and adaptation. Taylor and Francis, London, pp 443–480. https://doi.org/10.1007/978-1-4020-3218-9_12

Tani E, Kizis D, Markellou E, Papadakis I, Tsamadia D, Leventis G, Makrogianni D, Karapanos I (2018) Cultivar-dependent responses of eggplant (*Solanum melongena* L.) to simultaneous *Verticillium dahliae* infection and drought. Front Plant Sci 9:1181. https://doi.org/10.3389/fpls.2018.01181

Thalmann M, Santelia D (2017) Starch as a determinant of plant fitness under abiotic stress. New Phytol 214:943–951. https://doi.org/10.1111/nph.14491

Trifilò P, Raimondo F, Nardini A, Lo Gullo MA, Salleo S (2003) Drought resistance of *Ailanthus altissima*: root hydraulics and water relations. Tree Physiol 24:107–114. https://doi.org/10.1093/treephys/24.1.107

Trotta G, Savo V, Cicinelli E, Carboni M, Caneva G (2020) Colonization and damages of Ailanthus altissima (Mill.) Swingle on archaeological structures: evidence from the Aurelian Walls in Rome (Italy). Int Biodeterior Biodegrad 153:105054. https://doi.org/10.1016/j.ibiod.2020.105054

Turner NC, Long MJ (1980) Errors arising from rapid water loss in the measurement of leaf water potential by the pressure chamber technique. Aust J Plant Physiol 7:527–537

Walker GA, Robertson MP, Gaertner M, Gallien L, Richardson DM (2017) The potential range of *Ailanthus altissima* (tree of heaven) in South Africa: the roles of climate, land use and disturbance. Biol Invasions 19:3675–3690. https://doi.org/10.1007/s10530-017-1597-8

Wang JW, Wu J (2013) Effective elicitors and process strategies for enhancement of secondary metabolite production in hairy root cultures. Adv Biochem Engin Biotechnol 134:55–89

Webster CR, Jenksin MA, Jose S (2006) Woody invaders and the challenges they pose to forest ecosystems in the Eastern United States. J for 104:366–374. https://doi.org/10.1093/jof/104.7.366

Zhou J, Zeng L, Liu J, Xing D (2015) Manipulation of the xanthophyll cycle increases plant susceptibility to *Sclerotinia sclerotiorum*. PLoS Pathog 11(5):e1004878. https://doi.org/10.1371/journal.ppat.1004878